

Infrared Multiphoton Dissociation Spectra as a Probe of Ion Molecule Reaction Mechanism: The Formation of the Protonated Water Dimer via Sequential Bimolecular Reactions with 1,1,3,3-Tetrafluorodimethyl Ether

R. A. Marta* and T. B. McMahon*

Department of Chemistry, University of Waterloo, Waterloo, Ontario, Canada, N2L 3G1

T. D. Fridgen*

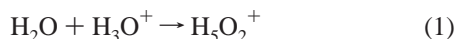
Department of Chemistry, Memorial University of Newfoundland, St. John's, Newfoundland, Canada, A1B 3X7

Received: March 20, 2007; In Final Form: May 30, 2007

The gas-phase ion–molecule reactions of 1,1,3,3-tetrafluorodimethyl ether and water have been examined using Fourier transform ion cyclotron resonance mass spectrometry, infrared multiphoton dissociation (IRMPD) spectroscopy, and ab initio molecular orbital calculations. This reaction sequence leads to the efficient bimolecular production of the proton-bound dimer of water (H_5O_2^+). Evidence for the dominant mechanistic pathway involving the reaction of $\text{CF}_2\text{H}-\text{O}=\text{CHF}^+$, an ion of m/z 99, with water is presented. The primary channel occurs via nucleophilic attack of water on the ion of m/z 99 ($\text{CF}_2\text{H}-\text{O}=\text{CHF}^+$), to lose formyl fluoride and yield-protonated difluoromethanol (m/z 69). Association of a second water molecule with protonated difluoromethanol generates a reactive intermediate that decomposes via a 1,4-elimination to release hydrogen fluoride and yield the proton-bound dimer of water and formyl fluoride (m/z 67). Last, the elimination of formyl fluoride occurs by the association of a third water molecule to produce H_5O_2^+ (m/z 37). The most probable isomeric forms of the ions with m/z 99 and 69 were found using IRMPD spectroscopy and electronic structure theory calculations. Thermochemical information for reactant, transition state, and product species was obtained using MP2(full)/6-311+G**//6-31G* level of theory.

Introduction

There has been a considerable effort recently in probing the gas-phase structure of the proton-bound dimer of water as well as other symmetric and asymmetric protonated dimers of small molecules using infrared multiphoton dissociation (IRMPD) spectroscopy.^{1–4} This has been accomplished by mating either a Fourier transform ion cyclotron resonance (FT-ICR)^{1–3} spectrometer or ion trap⁴ mass spectrometer to a tunable, infrared light source of high intensity, such as a free-electron laser (FEL). In an FT-ICR cell, the pressure is typically between 10^{-10} to 10^{-8} Torr. Under these low-pressure conditions it is difficult to produce weakly bound cluster ions such as the proton-bound dimer of water (eq 1) via direct ion–molecule association reactions since the number of collisions is very small during the lifetime of the complex.



Some years ago Clair and McMahon devised an elegant technique for the efficient production of H_5O_2^+ within the low-pressure confines of the FT-ICR cell.⁵ This method involved the addition of 1,1,3,3-tetrafluorodimethyl ether (TFDE) in the presence of water vapor directly into the FT-ICR cell. H_5O_2^+ is the dominant ionic species rapidly formed as the terminal ion–molecule reaction product. Electron impact (70 eV) on TFDE results almost exclusively in the formation of difluo-

romethyl cation at m/z 51, the result of cleavage of the C–O bond in the TFDE radical cation. This electrophilic species reacts quickly with TFDE by fluoride abstraction and elimination of fluoroform to yield an ion of m/z 99 that does not react further with TFDE (eq 2).

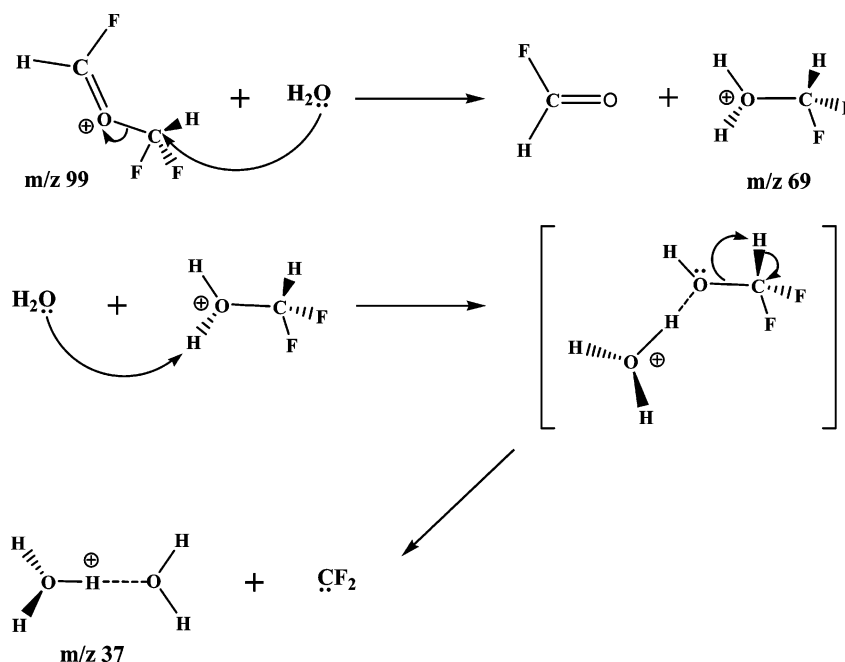


Addition of water to the ICR cell in which m/z 99 was the dominant ion resulted in facile formation of H_5O_2^+ . A mechanism for the formation of H_5O_2^+ was proposed in the work of Clair and McMahon⁵ in which it was suggested that m/z 99 undergoes $\text{S}_{\text{N}}2$ attack by water to form protonated difluoromethanol and formyl fluoride. Protonated difluoromethanol and water were then suggested to form a nascent proton-bound dimer that eliminates difluorocarbene to generate H_5O_2^+ (Scheme 1).⁵

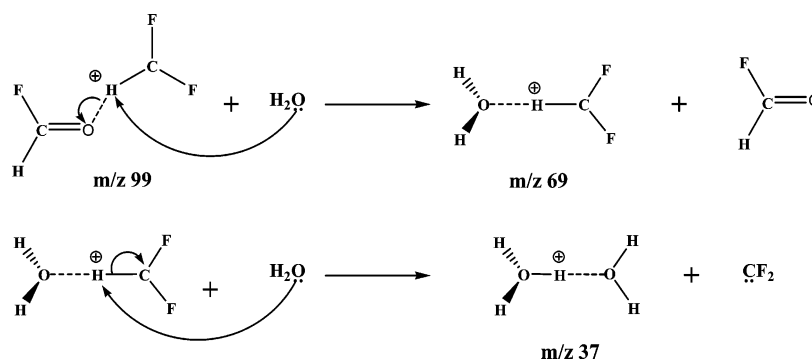
A second mechanism was proposed in which it was presumed that m/z 99 had the structure of a proton-bound dimer between difluorocarbene and formyl fluoride. Water then displaces formyl fluoride, producing a proton-bound dimer of water and difluorocarbene that then undergoes displacement of difluorocarbene by a second water molecule to yield H_5O_2^+ (Scheme 2).⁵ This second mechanism was proposed to account for the rapid production of H_5O_2^+ , because it involves a series of exchange reactions where H_2O acts as a stronger base that can displace both formyl fluoride and difluorocarbene. These reactions involving H_2O to form proton-bound dimers are then presumed to each occur at or near the collision rate.

* To whom all correspondence should be addressed. E-mail: (R.A.M.) ramarta@uwaterloo.ca; (T.B.M.) mcmahon@uwaterloo.ca; (T.D.F.) tfridgen@mun.ca.

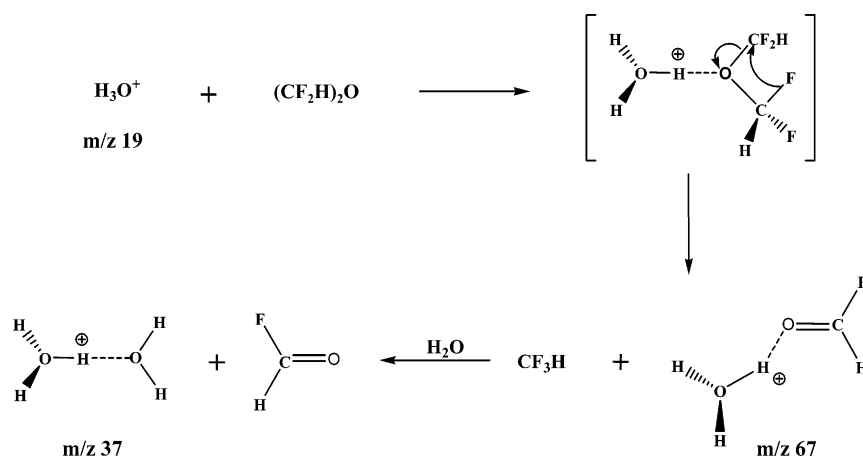
SCHEME 1



SCHEME 2



SCHEME 3



A third mechanism was also proposed which was not initiated by the m/z 99 ion, but rather a hydronium ion reacting with TFDE to produce the proton-bound dimer of formyl fluoride and water with the elimination of fluoroform. A second water molecule then displaces formyl fluoride to form $H_3O_2^+$ (Scheme 3).⁵

The schemes proposed by Clair and McMahon were based on evolution of ion intensities as a function of reaction time

obtained using conventional trapped-ion cyclotron resonance experiments. At the time of that work, the limited capabilities of the instrumentation did not allow for ion ejection to permit single-species ion isolation to be performed. The consequence of this inability to isolate a single ion of interest was that all possible ion–molecule reaction sequences occurred simultaneously. Therefore, several mechanistic arguments could be made to describe the observed time-intensity profiles. A further

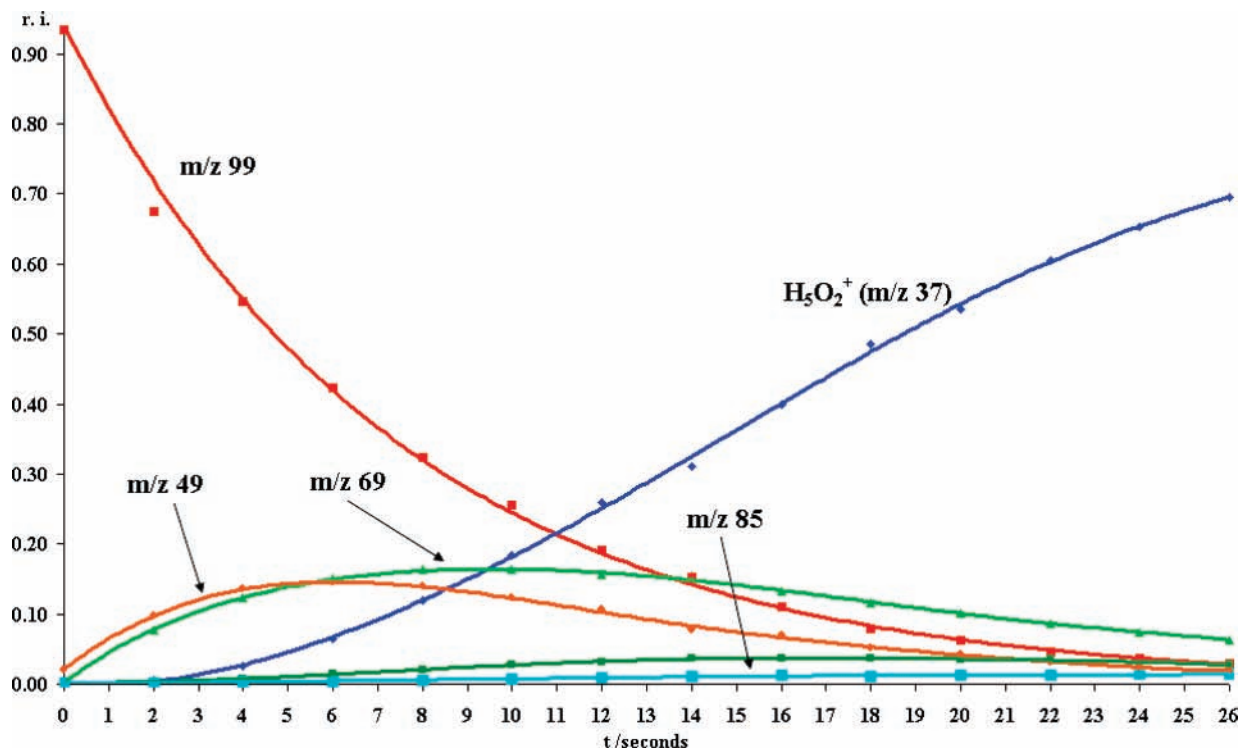


Figure 1. Relative intensity (ri) vs time profile produced by reaction of the ion with *m/z* 99 with water at partial pressure of 9.6×10^{-9} mbar.

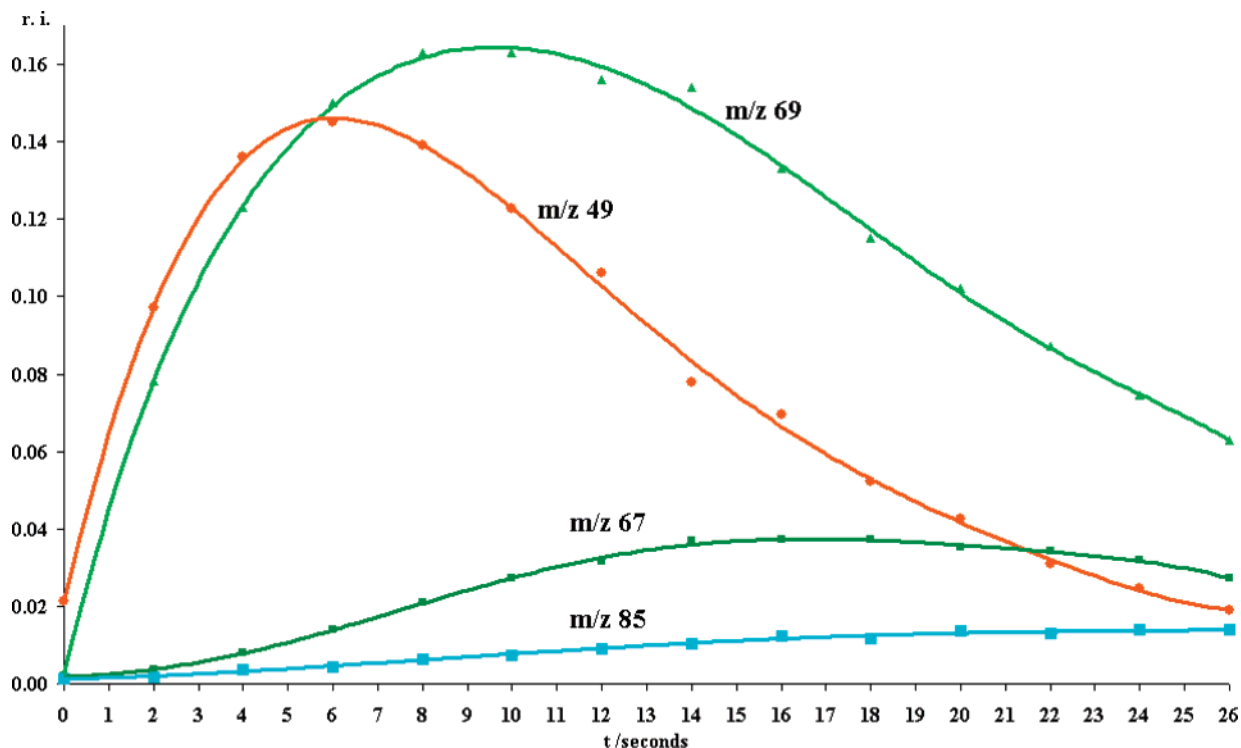


Figure 2. Relative intensity (ri) vs time profile for a selection of the low-intensity ions presented in the boxed region of Figure 1.

aid that was not readily available at that time was that of modern ab initio molecular orbital calculations and high-performance computing capabilities.

The present study incorporates the use of FT-ICR kinetics experiments, IRMPD spectroscopy, and ab initio calculations to better understand the novel ion-chemistry leading to bimolecular production of proton-bound dimers.

The application of the method using TFDE for efficiently generating H_5O_2^+ has been extrapolated to yield several examples of homogeneous and heterogeneous proton-bound

dimers formed within an FT-ICR apparatus designed specifically for IRMPD spectroscopy with the objective of structural characterization.²

Experimental Methods

FT-ICR Mass Spectrometry: Kinetic Studies. Experiments involving kinetic measurements were performed using a Spectrospin CMS 47 FT-ICR mass spectrometer, equipped with a 4.7 T, 150 mm horizontal bore superconducting magnet.

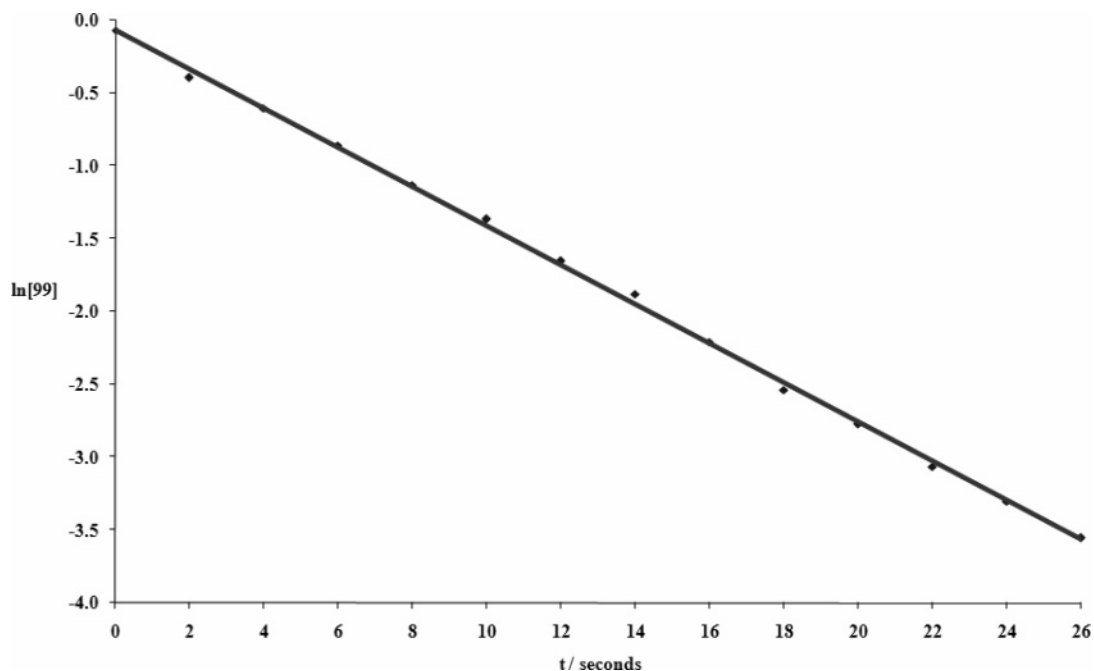


Figure 3. A plot of the natural logarithm of the relative intensity vs time for the ion with m/z 99 demonstrating pseudo-first-order kinetic behavior under a constant partial pressure of water.

Kinetics of bimolecular ion–molecule reactions are readily amenable to investigation with an FT-ICR experiment (eq 3).



The partial pressure of the neutral reactant molecule is carefully maintained constant via a molecular leak valve. If the partial pressure of the neutral (P_B) is held constant, then eq 3 may be expressed as a pseudo-first-order kinetic process with $k_{\text{obs}} = k_2 P_B$ (eq 4).



If the ion A^+ reacts via a pseudo-first-order kinetic process, then the differential equation for the instantaneous rate of change of the concentration of A^+ with respect to time is given by eq 5.

$$-\frac{d[A^+]}{dt} = k_{\text{obs}}[A^+] \quad (5)$$

Equation 5 can then be integrated to yield eq 6.

$$\ln[A^+] = -k_{\text{obs}}t \quad (6)$$

In this study, the quantity $[A^+]$ is the normalized ion intensity of A^+ . A plot of $\ln[A^+]$ versus t will yield a straight line with negative slope equal to the observed pseudo-first-order rate constant (k_{obs}/s^{-1}). The bimolecular rate constant (k_2/cm^3 molecules $^{-1}$ s $^{-1}$) associated with eq 3 can then also be obtained as shown by eq 7, where N_B is the number density of neutral reactant molecules, B.

$$k_2 = \frac{k_{\text{obs}}}{N_B} \quad (7)$$

The pressure of water reported here has been corrected for the sensitivity of the calibrated ionization gauge.

IRMPD Consequence Spectroscopy: Structural Elucidation. The coupling of the FT-ICR and free electron laser has been described previously. All IRMPD experiments were conducted at the Centre Laser Infrarouge d'Orsay (CLIO),⁶ which houses an FEL to which a mobile ion cyclotron resonance analyzer (MICRA)⁷ has been mated. IRMPD efficiency spectra are obtained by observing IRMPD of an ion of interest and all photoproducts of IRMPD as a function of radiation wavelength. The FEL wavelength was stepped in increments of ~ 5 cm $^{-1}$, and the laser bandwidth is 0.3–0.5% of the spectral wavelength. Ions were irradiated for 2 s. The laser wavelength and bandwidth are monitored via a monochromator associated with a spiricon multichannel detector. The ions were prepared directly within the ICR cell by electron-impact on 1,1,3,3-tetrafluorodimethyl ether, which was pulsed into the cell, and then allowed to react with water vapor, which was also subsequently pulsed into the ICR cell.

Computational Chemistry. Geometry optimization of all reactant and product species were performed at the MP2(full)/6-31G(d) level of theory. To obtain the enthalpies and thermal corrections required to calculate Gibbs free-energy changes of reaction, harmonic frequencies were determined at the same level of theory and scaled by 0.9427.⁸ Only minimum energy structures were used in calculations of thermochemical parameters. All optimized structures possessed no imaginary frequencies. For transition state structures, only one imaginary frequency associated with the mode connecting reactant and product species was present. The accuracy of the electronic energy calculation was further improved for all species by performing single-point calculations at the MP2(full)/6-311+G(d,p) level of theory.

To compare with experiment, infrared spectra were calculated using the B3LYP/6-31+G(d,p) level of theory. Density functional theory has been found to give very good agreement with gas-phase IRMPD in the past.^{1,2} The harmonic frequencies provided by the B3LYP/6-31+G(d,p) calculation were not scaled. All calculations were performed using the Gaussian 03 software package.⁹

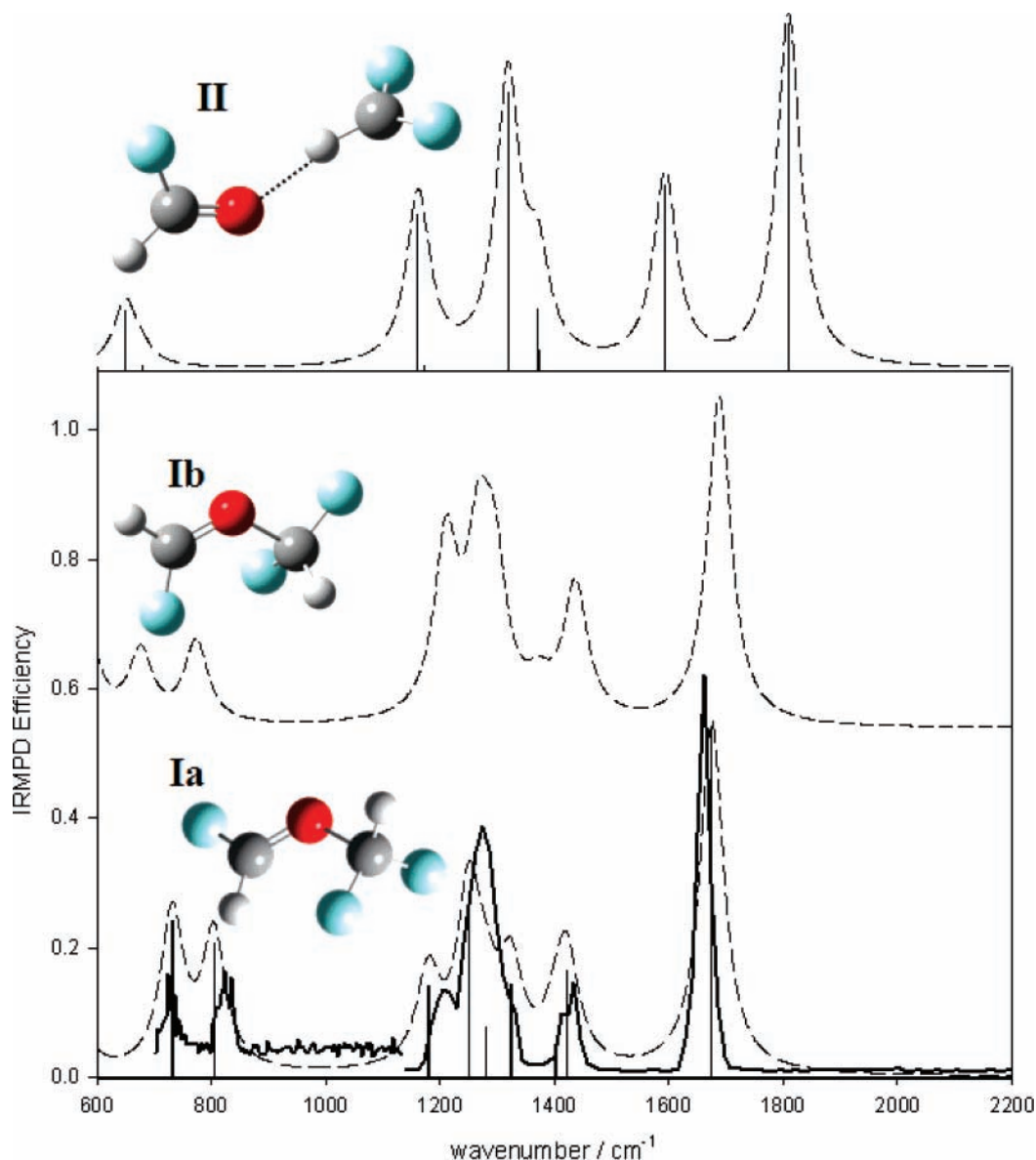


Figure 4. The IRMPD spectrum for the ion with m/z 99 is shown in the solid black line and a B3LYP/6-31+G** calculated spectrum is shown in the dashed black line for each of the species, Ia, Ib, and II. The ions Ia and Ib are two stable difluoromethylated formyl fluoride rotomers. The rotomer Ia is favored exergonically by 1.50 kJ mol^{-1} relative to Ib. The proton-bound dimer of difluorocarbene and formyl fluoride is species II.

Results and Discussion

The ability to trap and isolate single ions of interest allows for a partial kinetic evaluation of the mechanisms proposed by Clair and McMahon. A comparison of Schemes 1 and 2 reveals that the difference between the two mechanisms is the assumed structure of the ion of m/z 99 as well as the intermediate ion of m/z 69. In Scheme 1, it is proposed that m/z 99 has the structure of a difluoromethylated formyl fluoride ion, while Scheme 2 proposes that this species is a proton-bound dimer of formyl fluoride and singlet difluorocarbene. Similarly, Scheme 1 suggests that m/z 69 has the structure of protonated difluoromethanol, while Scheme 2 implicates a proton-bound dimer of water and difluorocarbene. In accordance with pseudo-first-order kinetics, under a constant partial pressure of water the sequences shown in Schemes 1 and 2 should exhibit first-order decay of m/z 99. The time-intensity profile for isolated m/z 99 in the presence of water and TFDE at a partial pressure of water of 9.6×10^{-9} mbar is shown in Figure 1. In addition to m/z 69, several other product ions are observed, and a selection of these ions is shown clearly in Figure 2.

The pseudo-first-order rate constant (k_{obs}) for the disappearance of m/z 99 is found to be $1.4 \times 10^{-1} \text{ s}^{-1}$ at a partial pressure of H_2O of 9.6×10^{-9} mbar (Figure 3), leading to a bimolecular rate constant for the reaction of m/z 99 with water of $6.0 (\pm 1.4) \times 10^{-10} \text{ cm}^3 \text{ molecules}^{-1} \text{ s}^{-1}$, which corresponds to approximately 22% of the ion–molecule collision rate.¹⁰

The structural identity of m/z 99 ($\text{C}_2\text{F}_3\text{H}_2\text{O}^+$) was interrogated using IRMPD spectroscopy and density functional theory calculations (Figure 4). IRMPD of m/z 99 revealed two dissociation pathways, loss of CF_3H and CO , that yields ions at m/z 29 and 71, respectively. The relative intensities of the two fragments slightly favored m/z 29, protonated carbon monoxide, over m/z 71, presumably protonated fluoroform. Both fragments probably result from an initial intramolecular transfer of fluoride to the CF_2H moiety resulting in loss of fluoroform (producing m/z 29) accompanied by near thermoneutral proton-transfer from HCO^+ to CF_3H such that the neutral loss is CO (producing m/z 71). According to NIST, the proton affinity (PA) of CF_3H is higher than that of CO by approximately 30 kJ mol^{-1} , which would suggest that the more abundant fragment

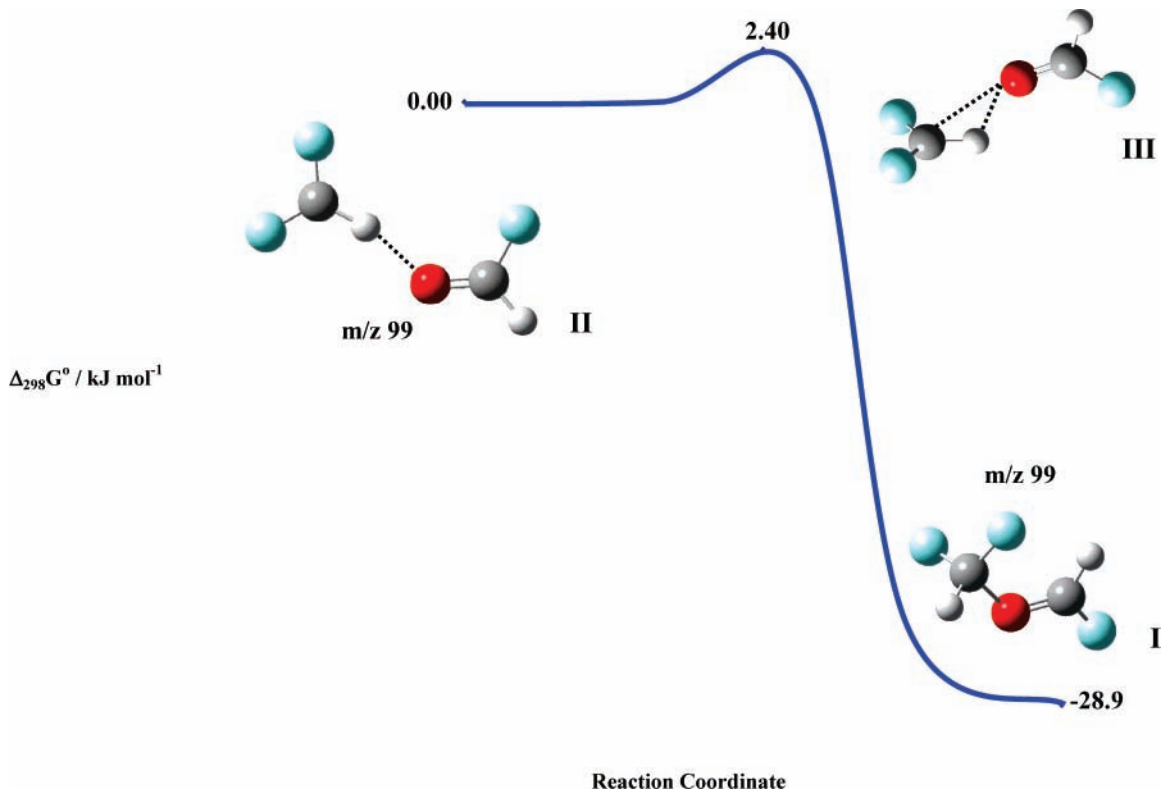


Figure 5. Gibbs free-energy (298 K) profile for the unimolecular isomerization of difluoromethylated formyl fluoride at m/z 99 (I) to the proton-bound dimer of difluorocarbene and formyl fluoride at m/z 99 (II) through a transition species (III).

ion should be m/z 71. The PA of CF_3H as reported by NIST is the same PA as that of CF_2H_2 of 620 kJ mol^{-1} , which raises considerable concern for the uncertainty of this reported value. Calculations at the CBS-Q^{11,12} level of theory find the PA of CF_3H and CF_2H_2 to be 562 kJ mol^{-1} and 542 kJ mol^{-1} , respectively. The preceding PA values are markedly different from the PA values of 620 kJ mol^{-1} reported by NIST. The calculated (CBS-Q) PA for CO is found to be 584 kJ mol^{-1} , which is in good agreement with the value reported by NIST of 590 kJ mol^{-1} . The CBS-Q calculations are thus consistent with observation of the dominant fragmentation of m/z 99 to yield protonated CO (HCO^+) at m/z 29 rather than protonated CF_3H at m/z 71. This demonstrates that caution should be taken with the NIST PA value reported for both CF_3H and CF_2H_2 .

The vibrational band assignments for the most probable isomer of m/z 99 (Ia) are shown in Table 1. The vibrational spectrum for ion m/z 99, species Ia, obtained by the electronic structure calculations is consistent with the IRMPD experiment. In addition, the calculations show that the difluoromethylated formyl fluoride (Ia) isomer is favored by 28.9 kJ mol^{-1}

TABLE 1: Band Assignments and Comparison of Predicted Band Positions for the IRMPD Spectrum of Isomer Ia of m/z 99, $\text{FHC}=\text{O}-\text{CF}_2\text{H}^+$

assignment	experimental band/ cm^{-1}	B3LYP/6-31+ G**/ cm^{-1}
C–O str	725	732
F–C=O bend	824	805
C–F str	1206	1180
C–F str	1275	1251
O–C–H bend		1280
H–C–F bend		1324
H–C=O bend	1434	1402
H–C–F bend (on CF_2H moiety)		1434
C=O str	1663	1675

over the proton-bound dimer of difluorocarbene and formyl fluoride (II) with a very small energy barrier of 2.40 kJ mol^{-1} separating the two (Figure 5). The difluoromethylated formyl fluoride isomer at m/z 99 Ia will be referred to as isomer I from here on.

The preceding evidence thus implies that the dominant structure of the ion with m/z 99 is difluoromethylated formyl fluoride (I). The ion is formed efficiently by reaction of difluoromethyl cation, the dominant fragment ion obtained by electron impact on TFDE, with TFDE to yield m/z 99 and fluoroform. Electronic structure calculations show this reaction (eq 2) to be exergonic by 124 kJ mol^{-1} (298 K).

Assuming the starting structure for m/z 99 is species Ia, as shown in Figure 4, it is then of interest to ascertain the most probable channel for the formation of H_5O_2^+ . In Scheme 1, the $\text{S}_{\text{N}}2$ displacement of formyl fluoride from m/z 99 via attack of water is calculated to be exergonic by 39.0 kJ mol^{-1} (298 K) and is shown in Figure 6. The bimolecular rate constant (k_2) for this reaction between water and m/z 99 of $6.0 (\pm 1.4) \times 10^{-10} \text{ cm}^3 \text{ molecules}^{-1} \text{ s}^{-1}$ is a significant fraction of the collision rate constant, implying an absence of any substantial barrier to reaction. This is in contrast to the smaller gas-phase bimolecular rate constants (300 K) measured for symmetric chloride¹³ and bromide¹⁴ gas-phase nucleophilic displacement reactions with rate constants at $3.5 (\pm 1.8) \times 10^{-14}$ and $2.4 (\pm 0.6) \times 10^{-11} \text{ cm}^3 \text{ molecules}^{-1} \text{ s}^{-1}$, respectively. The preceding symmetric exchange reactions are described generally by eq 8



and resemble the $\text{S}_{\text{N}}2$ reactions observed for positive ions such as the displacement of H_2O in the reaction of protonated methanol with methanol (eq 9). The rate constant obtained for

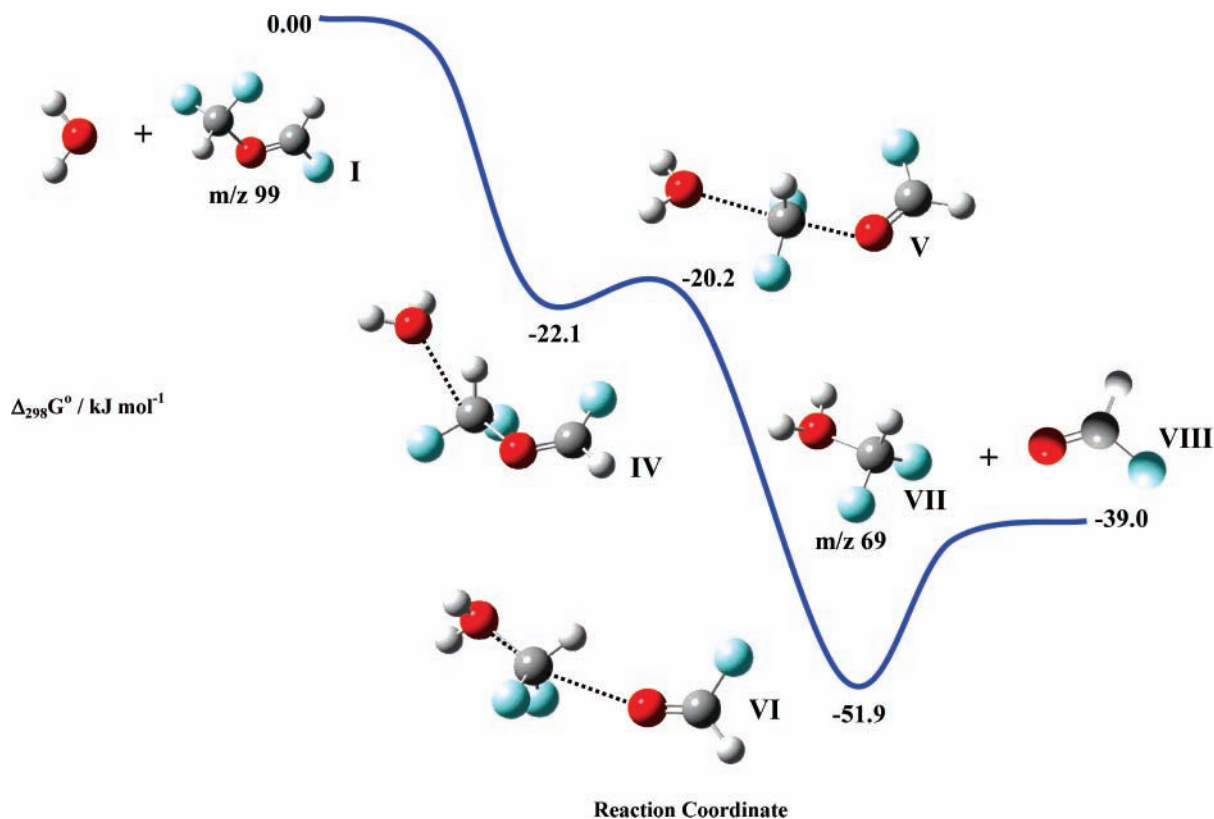
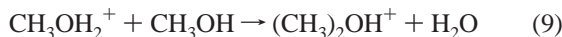


Figure 6. Gibbs free-energy (298 K) profile for the nucleophilic attack of water on difluoromethylated formyl fluoride with m/z 99 (I) to yield protonated difluoromethanol with m/z 69 (VII) and formyl fluoride (VIII).

the reaction described by eq 9 was found by McMahon and Beauchamp¹⁵ to be $1.05 \times 10^{-10} \text{ cm}^3 \text{ molecules}^{-1} \text{ s}^{-1}$. This was later verified by Fridgen and co-workers¹⁶ who obtained a value of $1.04 (\pm 0.02) \times 10^{-10} \text{ cm}^3 \text{ molecules}^{-1} \text{ s}^{-1}$. The rate constant determined in this work of $6.0 (\pm 1.4) \times 10^{-10} \text{ cm}^3 \text{ molecules}^{-1} \text{ s}^{-1}$ is on the same order of magnitude as the rate constants obtained in the above studies^{15,16} involving a positive ion as the electrophilic substrate.



Because the reaction of m/z 99 with water does not occur at collision rate, this provides further evidence that a displacement-type process involving proton transfer such as the one proposed in Scheme 2 is not likely. A reaction of this type would be expected to occur very close to or at the collision rate. The change in Gibbs free energy at 298 K for an $\text{S}_{\text{N}}2$ type mechanism proposed in the first step of Scheme 1 is shown in Figure 6.

The energetic pathway leading to formation of ions with m/z 49 and 69, whose time-intensity profiles are shown in Figure 2, is presented in Figure 6. The ions with m/z 49 and 69 are the protonated forms of formyl fluoride and difluoromethanol, respectively. The product ion is shown in Figure 6 exclusively as protonated difluoromethanol at m/z 69 (VII). It is feasible that protonated formyl fluoride with m/z 49 could be formed by simple proton transfer from the dissociating complex (VI). The difference in PA calculated at the CBS-Q^{11,12} level of theory is only 3.0 kJ mol^{-1} in favor of the protonation of difluoromethanol over formyl fluoride. The PA values calculated for difluoromethanol and formyl fluoride are 654 and 651 kJ mol^{-1} , respectively. It is thus reasonable to suggest that the proton will be statistically distributed between the two molecule entities.

The possibility of unimolecular isomerism between protonated difluoromethanol (VII) and the proton-bound dimer of difluo-

rocarbene and water (IX) was examined using electronic structure calculations. The proton-bound dimer of difluorocarbene and water (IX) was presented in Scheme 2. Protonated difluoromethanol (VII) is favored over the proton-bound dimer of difluorocarbene and water (IX) by 43.0 kJ mol^{-1} at 298 K (Figure 7). There is also a large barrier of isomerism from protonated difluoromethanol (VII) to the proton-bound dimer of difluorocarbene and water (IX) of 53.8 kJ mol^{-1} at 298 K (Figure 7). The protonated alcohol (VII) is both thermodynamically and kinetically favored over the proton-bound dimer (IX).

It was an unproductive effort to probe the structure of m/z 69 by IRMPD spectroscopy. This was due to protonated difluoromethanol at m/z 69 (VII) reacting rapidly with water resulting in an inadequate amount of isolation time for the ion to be irradiated by the laser. It was rationalized that a species analogous in structure to m/z 69, however less reactive, could be formed by reacting difluoromethylated formyl fluoride at m/z 99 (I) with dimethyl ether rather than water. This alternative reaction was performed and an oxonium ion with m/z 97 (B) was isolated and examined by IRMPD spectroscopy (Figure 8). By replacing the once acidic hydrogen atoms found attached to the oxygen in protonated difluoromethanol (VII) with methyl groups, the reactivity with water of the oxonium ion at m/z 97 (B) is reduced relative to protonated difluoromethanol at m/z 69 (VII). This reduced reactivity allowed the oxonium ion at m/z 97 (B) to be isolated readily for IRMPD analysis.

The vibrational band assignments for difluoromethylated dimethyl ether at m/z 97 (B) are given in Table 2.

IRMPD of difluoromethylated dimethyl ether at m/z 97 resulted in ionic products with m/z of 63 and 47, the latter being the slightly more dominant fragment. These ions are presumably methylated formyl fluoride (m/z 63) and protonated dimethyl ether (m/z 47) formed by loss of CH_3F and CF_2 , respectively. The latter fragmentation might have indicated a proton-bound

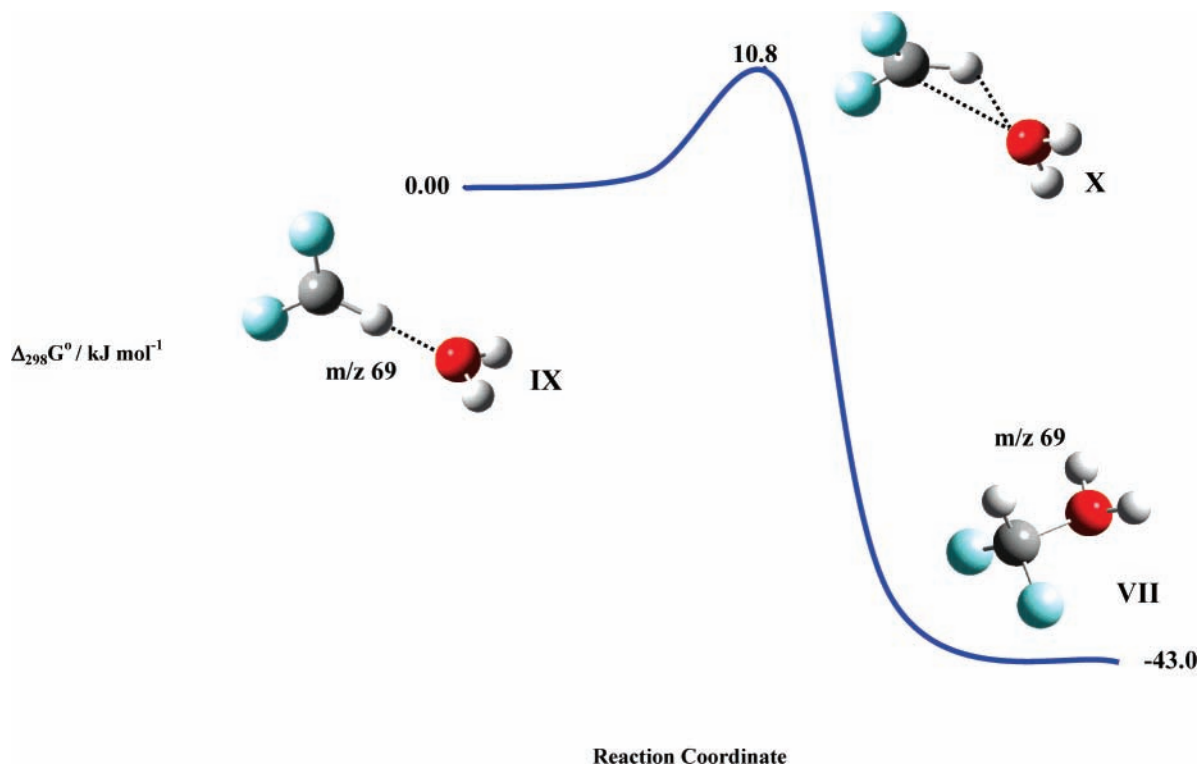


Figure 7. Gibbs free-energy (298 K) profile for the unimolecular isomerization of protonated difluoromethanol at m/z 69 (VII) to the proton-bound dimer of difluorocarbene and water at m/z 69 (IX) through a transition species (X).

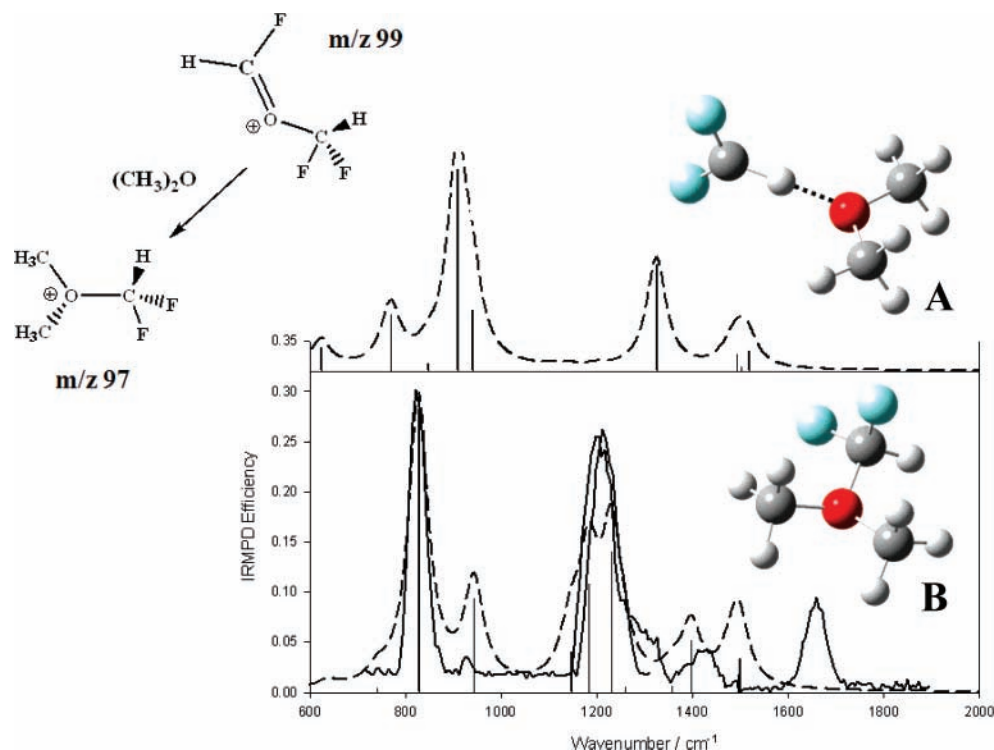


Figure 8. The IRMPD spectrum for the ion with m/z 97 (solid) and the B3LYP/6-31G* calculated spectra (dashed) for the proton-bound dimer of difluorocarbene and dimethyl ether (A) and a oxonium ion that can be described as difluoromethylated dimethyl ether (B).

dimer of difluorocarbene and dimethyl ether at m/z 97 (A). A comparison of the experimental infrared spectrum with the predicted spectra for the proton-bound dimer of difluorocarbene and dimethyl ether at m/z 97 (A) and difluoromethylated dimethyl ether at m/z 97 (B) reveals that the proton-bound dimer of difluorocarbene and dimethyl ether (A) is not a good candidate structure. The ion at m/z 47 is thus likely the result

of proton transfer from CF_2 to $(\text{CH}_3)_2\text{O}$ in the exit channel complex initiated by $\text{F}_2\text{HC}-\text{O}$ bond cleavage as shown by Scheme 4.

From a comparison of the experimental and predicted spectra, it is likely that the structure is the oxonium ion, difluoromethylated dimethyl ether, at m/z 97 (B). However, there is some disagreement between the experimental and predicted spectrum,

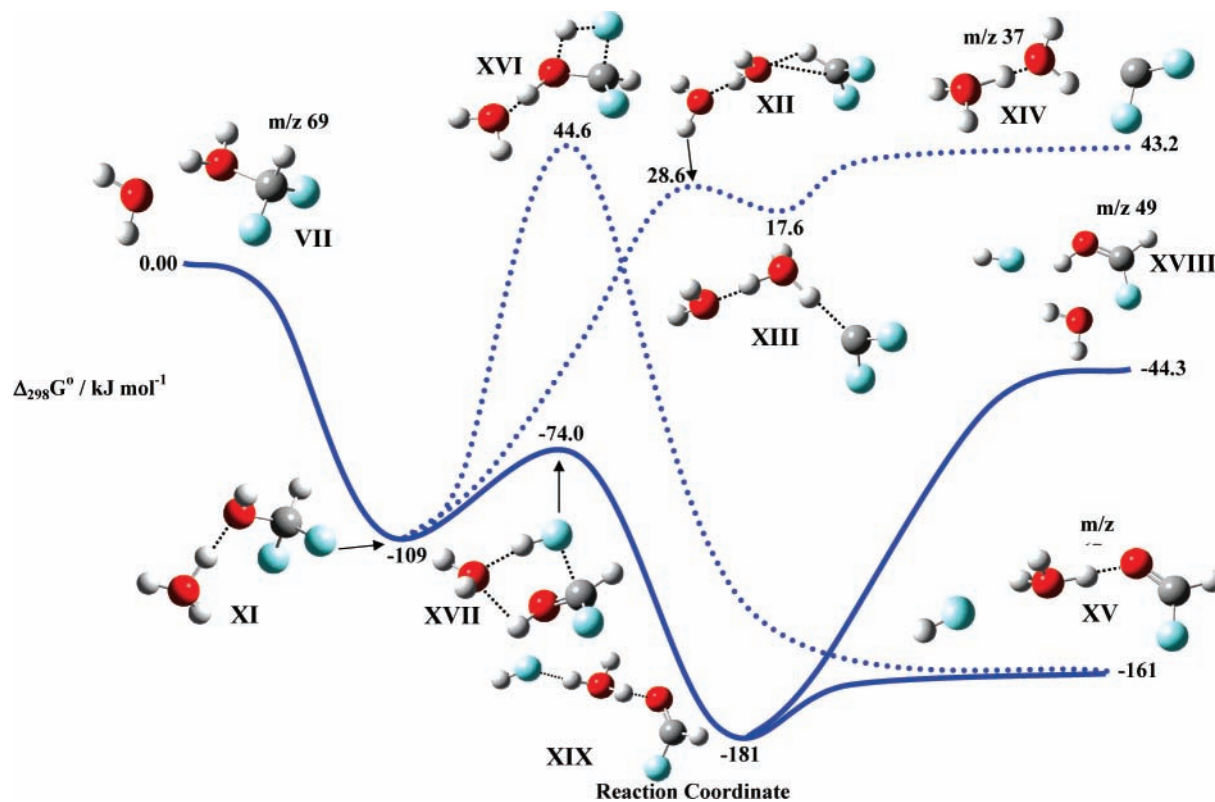
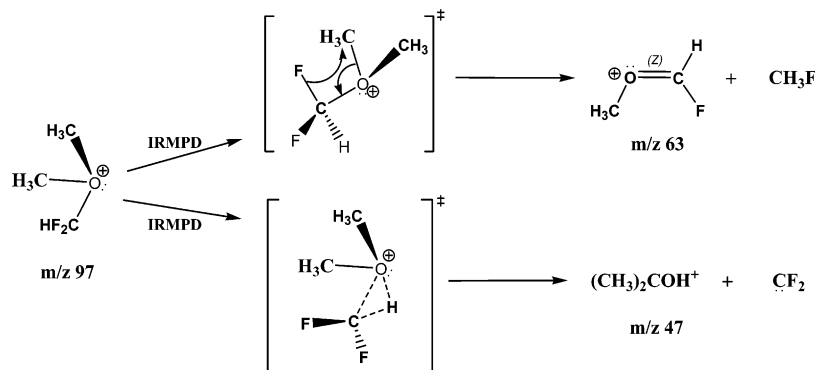


Figure 9. Gibbs free-energy (298 K) profile for the association of protonated difluoromethanol at m/z 69 (VII) with water to yield the proton-bound dimer of water and formyl fluoride at m/z 67 (XV) is shown in the solid blue line. Reaction processes that are endergonic relative to the reactants are shown in the dashed blue line.

SCHEME 4



especially in the 1500–1700 cm^{-1} region. The symmetric CH_3 deformation is predicted to occur at ~ 1500 cm^{-1} , which is typical for this mode. The observed position for this band could be that at either 1418 cm^{-1} or the higher energy at 1660 cm^{-1} . If the experimental band is not 1660 cm^{-1} , then it is difficult to account for it as there are not any other bands predicted to occur at higher energy other than the C–H stretches.

The spectra presented in Figure 8 shows that the identity of the ion with m/z 97 is more likely the difluoromethylated dimethyl ether (B) isomer rather than the proton-bound dimer of difluorocarbene and dimethyl ether (A). If formation of difluoromethylated dimethyl ether at m/z 97 (B) is analogous to the formation of protonated difluoromethanol at m/z 69 (VII), this then further justifies the assignment of protonated difluoromethanol at m/z 69 (VII) as the reactive isomer involved in the mechanism considered here.

The first step shown by Scheme 1 proposed by Clair and McMahon is supported experimentally and computationally. This is based on the evidence that there is an $\text{S}_{\text{N}}2$ attack of

water on the difluoromethylated formyl fluoride ion at m/z 99 (I) with a bimolecular rate coefficient of $6.0 (\pm 1.4) \times 10^{-10}$ $\text{cm}^3 \text{ molecules}^{-1} \text{ s}^{-1}$. The magnitude of the rate coefficient is consistent with an $\text{S}_{\text{N}}2$ process involving a positive ion as the electrophilic substrate.^{15,16} This reaction forms protonated difluoromethanol at m/z 69 predominantly but will also yield protonated formyl fluoride at m/z 49 (Figure 2). This is further evidence that the $\text{S}_{\text{N}}2$ process proposed for the first step of Scheme 1 by Clair and McMahon is a dominant reaction channel.

IRMPD spectroscopy has been used to directly identify the ion with m/z 99 as difluoromethylated formyl fluoride (I) and has been used to find the structure of the ion with m/z 69 as protonated difluoromethanol (VII). Identification of the structure of the ion with m/z 69 as protonated difluoromethanol (VII) was accomplished indirectly by isolation of an ion with m/z 97 formed analogously to protonated difluoromethanol (VII) by reacting dimethyl ether instead of water with difluoromethylated

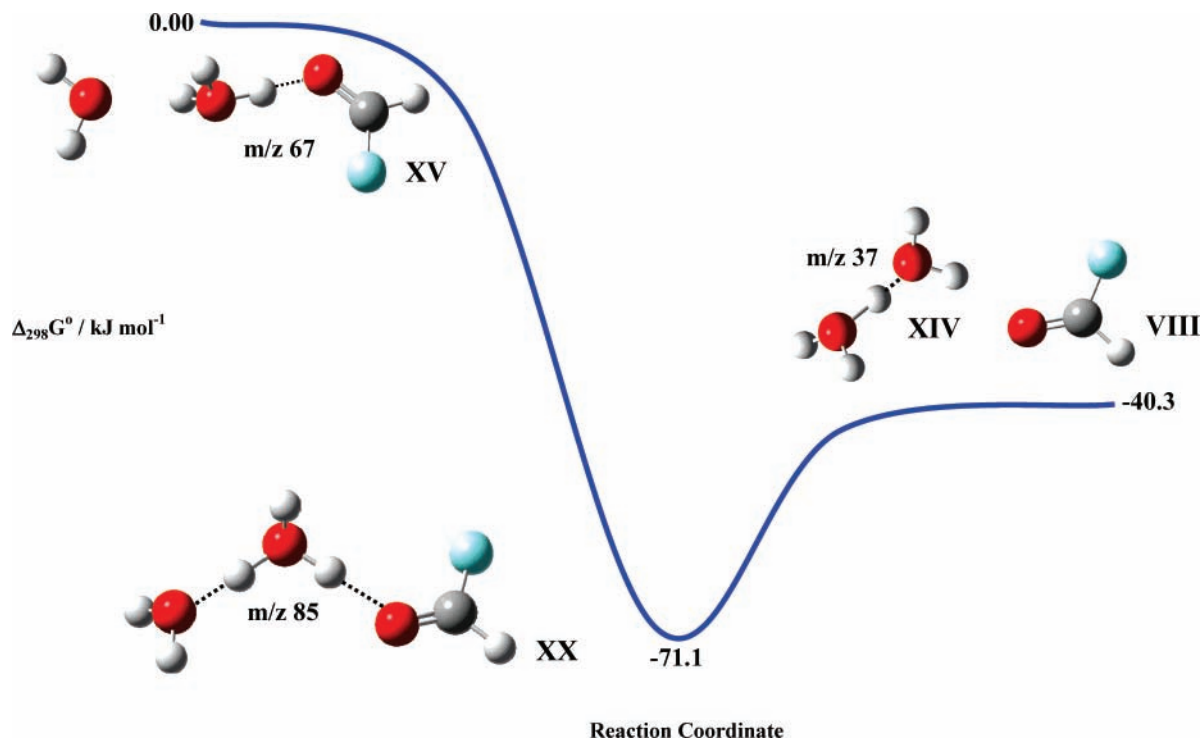


Figure 10. Gibbs free-energy (298 K) profile for the decomposition of the ion with m/z 85 (XX) into H_5O_2^+ at m/z 37 (XIV) and formyl fluoride (VIII).

TABLE 2: Band Assignments and Comparison of Predicted Band Positions for the IRMPD Spectrum of Species of m/z 97, $\text{HF}_2\text{CO}(\text{CH}_3)_2^+$ (B)

assignment	experimental band/ cm^{-1}	Ia, B3LYP/6-31+G**/ cm^{-1}
C–O str	822	828
C–O str	926	944
sym C–F str	1213	1148
C–F str		1184
C–F str		1233
H–C–F bend (?)	1418	1398
sym CH_3 def (?)	1660	1500

formyl fluoride (I). This species was an oxonium ion of difluoromethylated dimethyl ether at m/z 97 (B).

Electronic structure calculations at the MP2(full)/6-311+G-(d,p)/6-31G(d) level of theory show the $\text{S}_{\text{N}}2$ process presented in Scheme 1 to be exergonically favored at room temperature by 39.0 kJ mol^{-1} (Figure 6).

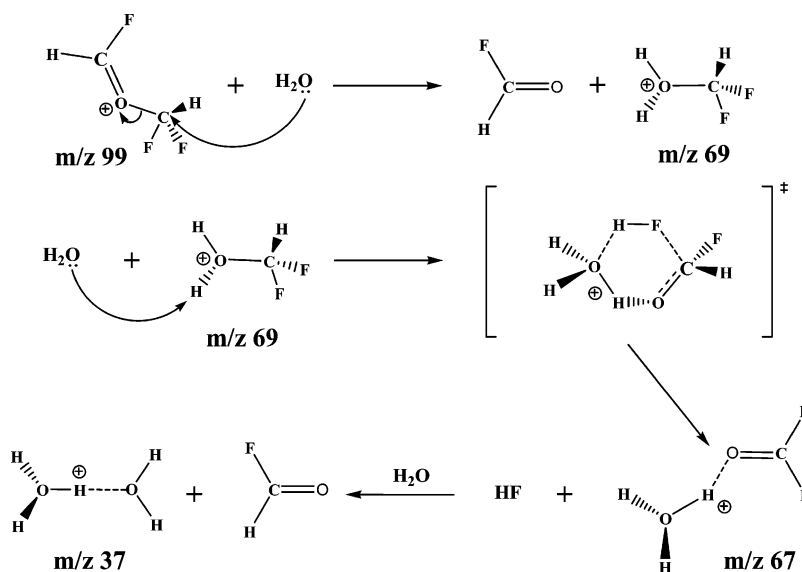
The second step proposed in Scheme 1 is formation of H_5O_2^+ at m/z 37 (XIV) and difluorocarbene from the reaction of protonated difluoromethanol at m/z 69 (VII) with water (Figure 9). This process is endergonic at 298 K by 43.2 kJ mol^{-1} (Figure 9) thus rendering this process most unlikely at room temperature. The barrier to decomposition is also relatively high and is 28.6 kJ mol^{-1} above the reactant species. The loss of difluorocarbene from ionic species has been previously observed in compounds containing trifluoromethyl groups,^{17–19} and thus it seems reasonable to assume also that it may be possible to lose difluorocarbene in compounds containing difluoromethyl groups. Because the loss of difluorocarbene from the water and protonated difluoromethanol complex (XI) is high-energy channel, it then suggests that a more energetically favorable channel is facilitating the rapid production of H_5O_2^+ . A feasible explanation for the elementary step leading to the formation of H_5O_2^+ is found by considering the two ions at m/z 67 and 85 as shown in Figure 2.

A possible source of the ion with m/z 67 is from the spontaneous decomposition of the complex formed by the reaction of water and protonated difluoromethanol (XI). This occurs by loss of hydrogen fluoride (HF) through a 1,4-elimination (XVII) transition state that is exergonic by 74.0 kJ mol^{-1} (298 K). The elimination of HF yields a proton-bound dimer of water and formyl fluoride at m/z 67 (XV) (Figure 9). It is not uncommon for ionic fluorine-containing species to lose HF, and this process has been investigated previously both experimentally and computationally.^{17,20,21} Following the configuration of the six member ring-like transition state (XVII), a ring-opened intermediate (XIX) is produced that can readily lose HF and yield the proton-bound dimer of water and formyl fluoride at m/z 67 (XV). The formation of the ring-opened intermediate (XIX) is exergonic by 181 kJ mol^{-1} (298 K). The production of HF and the proton-bound dimer of water and formyl fluoride at m/z 67 (XV) is exergonic by 161 kJ mol^{-1} (298 K).

A secondary channel to produce HF and the proton-bound dimer of water and formyl fluoride at m/z 67 (XV) was also considered. This secondary channel assumed a four member ring-like transition state (XVI) structure that proceeds through a 1,2-elimination of HF as opposed to the 1,4-elimination of HF proposed above. The 1,2-elimination was found to possess an endergonic barrier to decomposition of 44.6 kJ mol^{-1} (298 K), and it is thus not a kinetically accessible channel. The transition species (XVI) exhibits ring-strain, and this will cause it to be high in energy.

Following the production of the proton-bound dimer of water and formyl fluoride at m/z 67 (XV), a third water molecule may then associate with this ion to yield an ion at m/z 85 (XX) (Figure 10). This step is exergonic by 71.1 kJ mol^{-1} (298 K). The ion at m/z 85 (XX) can then decompose to produce H_5O_2^+ at m/z 37 (XIV) and formyl fluoride (VIII). The formation of H_5O_2^+ at m/z 37 (XIV) by the displacement of formyl fluoride (VIII) by water from the ion at m/z 85 (XX) is exergonic by 40.3 kJ mol^{-1} (Figure 10).

SCHEME 5



Conclusions

An efficient bimolecular process involving 1,1,3,3-tetrafluorodimethyl ether and water has been examined with FT-ICR mass spectrometry, IRMPD spectroscopy, and *ab initio* molecular orbital calculations.

The process involves the rapid production of the proton-bound dimer of water at $m/z\ 37$ ($H_5O_2^+$) (XIV). The dominant reaction channel occurs via the nucleophilic attack of water on difluoromethylated formyl fluoride at $m/z\ 99$ (I) to produce protonated difluoromethanol at $m/z\ 69$ (VII) and formyl fluoride (VIII). The bimolecular rate constant (k_2) for nucleophilic attack of water on difluoromethylated formyl fluoride at $m/z\ 99$ (I) was found to be $6.0 (\pm 1.4) \times 10^{-10} \text{ cm}^3 \text{ molecules}^{-1} \text{ s}^{-1}$. The rate of nucleophilic attack is of the same order of magnitude as previously measured systems involving positive ions as an electrophilic substrate.^{15,16}

Association of a second water molecule with protonated difluoromethanol at $m/z\ 69$ (VII) leads to decomposition via the 1,4-elimination of hydrogen fluoride (XVII) to form the proton-bound dimer of water and formyl fluoride at $m/z\ 67$ (XV). Finally, the displacement of formyl fluoride occurs by the association of a third water molecule with the proton-bound dimer of water and formyl fluoride at $m/z\ 67$ to yield $H_5O_2^+$ at $m/z\ 37$ (XIV) (Scheme 5).

IRMPD spectroscopy and density functional theory calculations have been used to determine the most probable structure of the ions observed at $m/z\ 99$ and 69. The ions with $m/z\ 99$ and 69 are difluoromethylated formyl fluoride (I) and protonated difluoromethanol (VII), respectively.

Electronic structure calculations at the MP2(full)/6-311+G-(d,p)/6-31G(d) level of theory show that the exergonicity of the sequential reaction steps as proposed by Scheme 5 facilitate the abundant formation of $H_5O_2^+$ (XIV).

Acknowledgment. The generous financial support of the Natural Sciences and Research Council of Canada is gratefully acknowledged in the form of research grants to T.D.F. (Memorial) and T.B.M. (Waterloo) as well as a post-graduate scholarship to R.A.M.. The assistance of the CLIO team including P. Maitre, J. Lemaire, L. MacAleese, and J. M. Ortega is gratefully acknowledged. We would also like to thank Gerard Mauclaire, Michel Heninger, Gerard Bellec, Pierre Boissel, and Joel Lemaire for providing MICRA (the mobile FT-ICR) used in this work.

References and Notes

- (1) Fridgen, T. D.; McMahon, T. B.; MacAleese, L.; Lemaire, J.; Maitre, P. *J. Phys. Chem. A* **2004**, 9008.
- (2) Fridgen, T. D.; MacAleese, L.; Maitre, P.; McMahon, T. B.; Boissel, P.; Lemaire, J. *Phys. Chem. Chem. Phys.* **2005**, 7, 2747.
- (3) Fridgen, T. D.; MacAleese, L.; McMahon, T. B.; Lemaire, J.; Maitre, P. *Phys. Chem. Chem. Phys.* **2006**, 8, 955.
- (4) Asmis, K. R.; Pivonka, N. L.; Santambrogio, G.; Brümmer, M.; Kaposta, C.; Neumark, D. M.; Wöste, L. *Science* **2003**, 299, 1375.
- (5) Clair, R. L.; McMahon, T. B. *Can. J. Chem.* **1980**, 58, 863.
- (6) Prazeres, R.; Glotin, F.; Insa, C.; Jaroszynski, D. A.; Ortega, J. *Eur. Phys. J. D* **1998**, 87.
- (7) Mauclaire, G.; Lemaire, J.; Boissel, P.; Bellec, G.; Heninger, M. *Eur. J. Mass Spectrom.* **2004**, 10.
- (8) Foresman, J. B.; Frisch, A. *Exploring Chemistry with Electronic Structure Methods*, 2nd ed.; Gaussian Inc.: Pittsburgh, PA, 1996.
- (9) Frisch, M. J.; Trucks, G. W.; Schlegel, H. B.; Scuseria, G. E.; Robb, M. A.; Cheeseman, J. R.; Montgomery, J. A., Jr.; T. V.; Kudin, K. N.; Burant, J. C.; Millam, J. M.; Iyengar, S. S.; Tomasi, J.; Barone, V.; Mennucci, B.; Cossi, M.; Scalmani, G.; Rega, N.; Petersson, G. A.; Nakatsuji, H.; Hada, M.; Ehara, M.; Toyota, K.; Fukuda, R.; Hasegawa, J.; Ishida, M.; Nakajima, T.; Honda, Y.; Kitao, O.; Nakai, H.; Klene, M.; Li, X.; Knox, J. E.; Hratchian, H. P.; Cross, J. B.; Adamo, C.; Jaramillo, J.; Gomperts, R.; Stratmann, R. E.; Yazyev, O.; Austin, A. J.; Cammi, R.; Pomelli, C.; Ochterski, J. W.; Ayala, P. Y.; Morokuma, K.; Voth, G. A.; Salvador, P.; Dannenberg, J. J.; Zakrzewski, V. G.; Dapprich, S.; Daniels, A. D.; Strain, M. C.; Farkas, O.; Malick, D. K.; Rabuck, A. D.; Raghavachari, K.; Foresman, J. B.; Ortiz, J. V.; Cui, Q.; Baboul, A. G.; Clifford, S.; Cioslowski, J.; Stefanov, B. B.; Liu, G.; Liashenko, A.; Piskorz, P.; Komaromi, I.; Martin, R. L.; Fox, D. J.; Keith, T.; Al-Laham, M. A.; Peng, C. Y.; Nanayakkara, A.; Challacombe, M.; Gill, P. M. W.; Johnson, B.; Chen, W.; Wong, M. W.; Gonzalez, C.; Pople, J. A. *Gaussian 03, revision C.02*; Gaussian, Inc.: Wallingford, CT, 2004.
- (10) Su, T.; Chesnavich, W. J. *J. Chem. Phys.* **1982**, 76, 5183.
- (11) Ochterski, J. W.; Petersson, G. A.; Montgomery, J. A., Jr. *J. Chem. Phys.* **1996**, 104, 2598.
- (12) Montgomery, J. A., Jr.; Frisch, M. J.; Ochterski, J. W.; Petersson, G. A. *J. Chem. Phys.* **1999**, 110, 2822.
- (13) Barlow, S. E.; VanDoren, J. M.; Bierbaum, V. M. *J. Am. Chem. Soc.* **1988**, 110, 7240.
- (14) Viggiano, A. A.; Morris, R. A.; Paschkewitz, J. S.; Paulson, J. F. *J. Am. Chem. Soc.* **1992**, 114, 10477.
- (15) Beauchamp, J. L.; McMahon, T. B. *J. Phys. Chem.* **1977**, 81, 593.
- (16) Fridgen, T. D.; Keller, J. D.; McMahon, T. B. *J. Phys. Chem. A* **2001**, 105, 3816.
- (17) Sekiguchi, O.; Watanabe, D.; Nakajima, S.; Tajima, S.; Uggerud, E. *Int. J. Mass Spec.* **2003**, 222, 1.
- (18) Wesdemiotis, C.; Schwarz, H.; Budzikiewicz, H.; Vogel, E. *Org. Mass Spectrom.* **1981**, 16, 89.
- (19) Tajima, S.; Takahashi, S.; Sekiguchi, O. *Rapid Commun. Mass Spectrom.* **1999**, 13, 1458.
- (20) Carhini, M.; Conte, L.; Gambaretto, G.; Catinella, S.; Traldi, P. *Org. Mass Spectrom.* **1992**, 27, 1248.
- (21) Várnai, P.; Nyulási, L.; Veszprémi, T.; Vékey, K. *Chem. Phys. Lett.* **1995**, 233, 340.